Journal of Biochemistry and Molecular Biology, Vol. 37, No. 5, September 2004, pp. 565-573

JOURNAL OF Biochemistry and Molecular Biology

Solution Structure of Human Orexin-A: Regulator of Appetite and Wakefulness

Hai-Young Kim[†], Eunmi Hong[†], Jae-il Kim[‡] and Weontae Lee[†,*]

[†]Department of Biochemistry, College of Science, Yonsei University, Seoul 120-740, Korea

[‡]Anygen Co., Kwangju 500-712, Korea

Received 30 October 2003, Accepted 24 February 2004

Orexin-A and orexin-B (hypocretin-1 and hypocretin-2, respectively) are important hypothalamic neuro-peptides, which are encoded by a single mRNA transcript and stimulate food intake as well as regulate wakefulness. Here we determined the solution structure of orexin-A by NMR spectroscopy and by simulated-annealing calculation. The structural features of orexin-A involve two α-helices, with the hydrophobic residues disposed to on one side of helix, and hydrophilic residues to the other. A hydrophilic turn induced by two disulfide bonds provides the key difference between orexin-A and -B. With previous mutagenic studies, the derived structure of orexin-A provides us with a structure-functional view for novel drug design.

Keywords: Neuropeptide, NMR, Obesity, Orexin-A, Solution structure

Introduction

The most abundant mammalian neuro-peptides characterized to date are involved in a multiplicity of the physiological functions, namely, thermoregulation, obesity, blood pressure, cardiovascular system (Murphy *et al*., 1983; De Wied *et al*., 1991; Smith *et al*., 1992; Li *et al*., 1996; Fan *et al*., 1997; de Lecea *et al*., 1998; Sakurai *et al*., 1998; Willie *et al*., 2001). It has been reported that the peptides orexin-A and orexin-B (also called hcrt-1 and hcrt-2) are involved in a number of cell signal-transduction pathways, for example, feeding behavior and energy homeostasis (Sakurai *et al*., 1998; de Lecea *et al*., 1998). Feeding behavior depends on a multiplex of metabolic, autonomic, endocrine, and environmental factors, which are coordinated by an appropriate state of cortical arousal (wakefulness). It has been reported that since orexin peptides have something to do with the sleep cycle, that a deficiency of orexin peptides generates narcoleptic symptoms (Willie *et al*., 2001).

The mRNA of the precursor of these orexins was specifically found in the lateral hypothalamus and adjacent areas, which are extensively involved in the integrated processes that regulate feeding behavior and energy homeostasis (Bernardis *et al*., 1993; Bernardis *et al*., 1996). However, a recent report demonstrated orexin-A expression in human peripheral tissues (Nakabayashi *et al*., 2003). The orexin peptides are produced by the proteolytic cleavage of an oligo-peptide precursor, prepro-orexin, and both N-terminal pyroglutamyl cyclic forms, orexin-A and C, which are terminal amidation variants of these two peptides, are frequently found as post-translational modification products. Orexin-A, a 33-residue peptide, contains two disulfide bonds, whereas orexin-B, a 28-residue peptide, does not possess a cysteine residue, even though it has 46% sequence identity with orexin-A (Fig. 1). Vertebrate orexin peptides show high sequence homology. Orexin peptides cloned from the amphibian *Xenopus laevis* were found to have high sequence homology with their mammalian counterparts (Willie *et al*., 2001). In addition, both human and rat orexin receptors have been recognized as members of the seven-transmembrane protein family of orphan G-protein-coupled cell surface receptors (Sakurai *et al*., 1998).

Orexin peptides stimulate food consumption and their production is regulated by nutritional state. NMR studies on several neuro-peptides have already provided convincing evidence concerning the importance of structure in the central

Abbreviations: NMR, nuclear magnetic resonance; CD, circular dichroism; NOE, nuclear overhauser effect; DG, distance geometry; SA, simulated-annealing; REM, restraint energy minimization; RMSD, root-mean-square deviation; TOCSY, total correlation spectroscopy; DQF-COSY, double quantum filtered correlation spectroscopy; *h*OX1R, human orexin-1 receptor; *h*OX2R, human orexin-2 receptor

*To whom correspondence should be addressed.
Tel: 82-2-2123-2706; Fax: 82-2-363-2706
E-mail: wlee@spin.yonsei.ac.kr

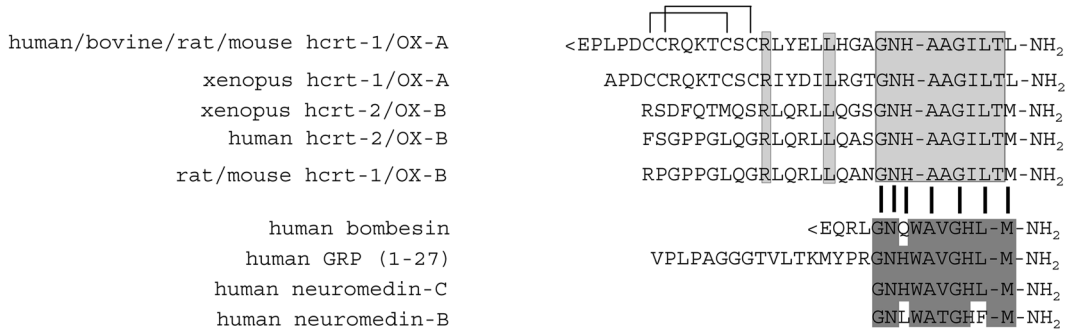

Fig. 1. Alignment of the amino acid sequences of hypocretins/orexins and of the bombesin family residue in the carboxy-terminus. The topologies of the two disulfide bonds in human orexin-A are indicated on the sequence. Identical residues are boxed. The N-terminus of human orexin-A is a pyroglutamyl residue (< E).

regulation of obesity and energy balance (Darbon *et al.*, 1992; Monks *et al.*, 1996). We previously reported that human orexin-B forms two α-helices connected by a small linker (Lee *et al.*, 1999). Here, we present the three-dimensional solution structure of human orexin-A as determined by two-dimensional NMR spectroscopy and dynamical simulated-annealing calculation. In terms of comparing it with the human orexin-B structure, we describe the characteristics of the human orexin-A structure-function relationship. This study adds information on the structure-function relationships of orexin-A, and provides a structural background for further ligand-receptor recognition studies on orexin neuropeptides.

Materials and methods

Peptide synthesis and purification Human orexin-A(Ac-Glu[1]-Pro[2]-Leu[3]-Pro[4]-Asp[5]-Cys[6]-Cys[7]-Arg[8]-Gln[9]-Lys[10]-Thr[11]-Cys[12]-Ser[13]-Cys[14]-Arg[15]-Leu[16]-Tyr[17]-Glu[18]-Leu[19]-Leu[20]-His[21]-Gly[22]-Ala[23]-Gly[24]-Asn[25]-His[26]-Ala[27]-Ala[28]-Gly[29]-Ile[30]-Leu[31]-Thr[32]-Leu[33]-NH_2) was synthesized commercially (Anygen Co., Kwangju, Korea). The linear resin-bound peptide was synthesized as described above with Cys (Acm) in positions 6 and 12 and Cys (Trt) in positions 7 and 14. The synthetic peptide was purified by reverse-phase liquid chromatography using a Shim-Pack C18 column on a Water Delta Prep 4000 system. The disulfide bonded form of the peptide was characterized by the combined use of HPLC and MALDI-TOF mass spectrometry and confirmed by NMR spectroscopy: ββ NOE between disulfide-bonded cysteine residues shown in Fig. 1 (Werner *et al.*, 1993).

Circular dichroism spectroscopy CD spectra of 80 μM human orexin-A were measured in 50 mM potassium phosphate buffer at various pHs, temperatures, and micelle conditions using a Jasco J-810 spectropolarimeter. CD spectra were recorded from 190 to 250 nm at a scanning rate of 50 nm/min with a time constant of 0.5 sec. Each CD spectrum was obtained by averaging 10 recordings with a step resolution of 0.2 nm and a bandwidth of 2.0 nm in cells with 0.1 mm path length (Koo *et al.*, 2002).

NMR spectroscopy NMR was performed upon 2 mM of the peptide in 50 mM potassium phosphate buffer at pH 7.0 in 100% D_2O and 90% H_2O/10% D_2O. NMR spectra were recorded at 278 K on Bruker DRX-500 and DRX-600 spectrometers equipped with a triple-resonance probe and an x, y, z-shielded pulsed-field

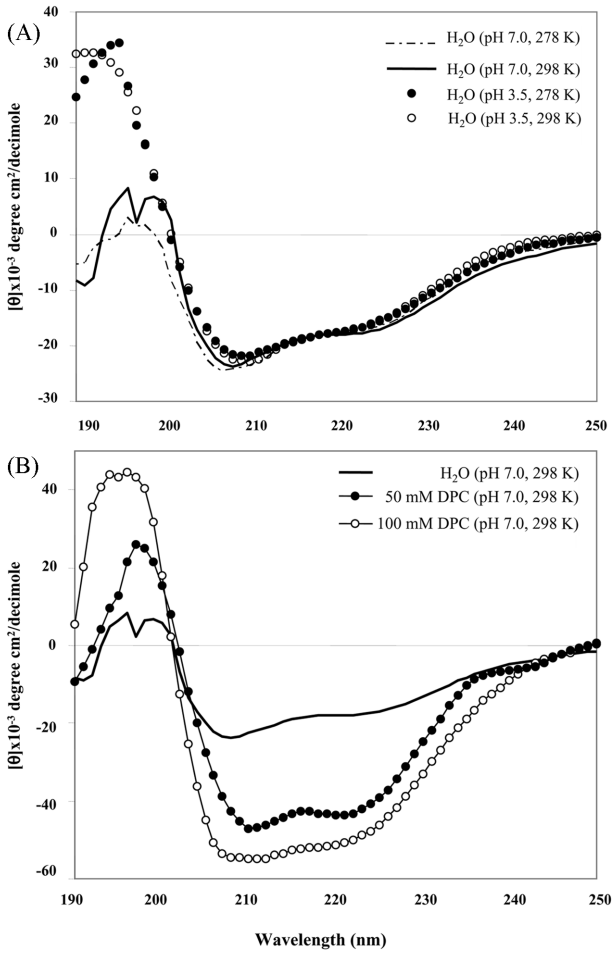

Fig. 2. Circular dichroism spectra of human orexin-A in various conditions; (A) H_2O at pH 7.0, 278 K (dash line), H_2O at pH 7.0, 298 K (black line), H_2O at pH 3.5, 278 K (closed circle), H_2O at pH 3.5, 298 K (open circle). (B) H_2O at pH 7.0, 298 K (black line), 50 mM DPC at pH 7.0, 298 K (closed circle and line), 100 mM DPC at pH 7.0, 298 K (open circle and line).

gradient coil. Two-dimensional (2D) NMR spectra were recorded in the phase-sensitive mode using time-proportional phase incrementation (Marion *et al*., 1983) for quadrature detection in the t_1 domain. 2D experiments were performed using double-quantum-filtered COSY (DQF-COSY) (Rance *et al*., 1983), TOCSY (Davis *et al*., 1985) using a MLEV-17 spin-lock pulse sequence and a mixing time of 69.7 ms, and NOESY (Jeener *et al*., 1979) with mixing times of 200, 300, 400, 600 ms. For the DQF-COSY experiments, solvent suppression was performed by selective low-power irradiation of water resonance during the 2.0 s of relaxation delay. Solvent suppression for TOCSY and NOESY was achieved using a WATERGATE pulse sequence (Piotto *et al*., 1992) combined with a pulsed-field gradient pulse. All NMR spectra were acquired with 2048 complex data points in the t_2 and 256 increments in the t_1 dimension, with 32 scans per increment. Slowly exchanging amide protons were identified by lyophilizing fully protonated samples in H_2O solutions, redissolving these in 100 % D_2O, and immediately acquiring a series of one-dimensional NOESY and 2D-NOESY spectra. $^3J_{HN\alpha}$ coupling constants were determined from 2D-DQF-COSY spectra, and strip-transformed to 8 K × 1 K.

All NMR data were processed on a Silicon Graphics Indigo II workstation using nmrPipe/nmrDraw (Delaglio *et al*., 1995) or XWIN-NMR (Bruker Instruments, Karlsruhe, Germany) software and analyzed using the Sparky 3.60 program (Goddard *et al*., 2003). Proton chemical shifts were expressed relative to the methyl resonance of internal sodium 2, 2-dimethyl-2-silapentane-5-sulfonic acid (DSS).

Structural restraints and structure calculations Distance restraints were derived from NOESY spectra in 90 % H_2O/10% D_2O solution. A total of 211 NOE constraints, 16 backbone

Table 1. Proton NMR chemical shift assignments for human orexin-A in 90% H_2O/10% D_2O solution

Residues	NH	$C^{\alpha}H$	$C^{\beta}H$	Others
Glu1	7.707	3.964	1.653	$C^{\gamma}H_2$ (2.094)
Pro2		4.161	1.980	$C^{\gamma}H_2$ (1.710,1.587) $C^{\delta}H_3$ (3.441)
Leu3	8.208	4.243	1.191	$C^{\gamma}H$ (1.191) $C^{\delta}H_3$ (0.623)
Pro4		4.155	1.980	$C^{\gamma}H_2$ (1.724, 1.592) $C^{\delta}H_3$ (3.408)
Asp5	7.789	4.281	2.462, 2.362	
Cys6	7.858	4.053	2.816	
Cys7	8.910	4.492	2.998	
Arg8	8.284	3.931	1.482	$C^{\gamma}H_2$ (1.282) $C^{\delta}H_2$ (2.904) N_2H (7.412,6.714)
Gln9	8.166	4.264	1.575	$C^{\gamma}H_2$ (2.033) $N^{\delta}H_2$
Lys10	7.757	3.944	1.243	$C^{\gamma}H_2$ (1.019) $C^{\delta}H_2$ (2.979) $C^{\varepsilon}H_2$ $N^{\varepsilon}H_3^+$ (7.944)
Thr11	8.139	4.043	3.659	$C^{\gamma}H_3$ (1.107)
Cys12	7.434	3.762	2.494	
Ser13	8.457	4.158	3.575	
Cys14	8.498	4.201	2.356	
Arg15	7.674	3.798	1.653	$C^{\gamma}H_2$ (1.362) $C^{\delta}H_2$ (2.909) NH_2 (6.615,7.316)
Leu16	8.231	4.174	1.334	$C^{\gamma}H$ (1.334) $C^{\delta}H_3$ (0.597)
Tyr17	7.982	4.353	2.901, 2.570	2,6H(7.412) 3,5H(6.938)
Glu18	8.057	3.727	1.765	$C^{\gamma}H_2$ (2.054)
Leu19	7.801	3.907	1.544	$C^{\gamma}H$ (1.279) $C^{\delta}H_3$ (0.874,0.573)
Leu20	7.801	3.907	1.544	$C^{\gamma}H$ (1.279) $C^{\delta}H_3$ (0.874,0.573)
His21	7.614	4.276	2.801	2H (7.864) 4H (6.843)
Gly22	8.406	4.087		
Ala23	8.289	4.335	1.051	
Gly24	8.303	3.656		
Asn25	8.080	4.416	2.449	$N^{\gamma}H_2$
His26	8.222	4.380	2.870	2H (7.783) 4H (6.615)
Ala27	8.322	4.239	1.245	
Ala28	7.955	3.896	1.255	
Gly29	8.530	4.276		
Ile30	7.479	4.073	1.902	$C^{\gamma}H_2$ (1.757) $C^{\gamma}H_3$ (1.482) $C^{\delta}H_3$ (1.097)
Leu31	8.110	4.064	1.339	$C^{\gamma}H$ (1.339) $C^{\delta}H_3$ (0.581)
Thr32	7.997	4.116	3.927	$C^{\gamma}H_3$ (0.875)
Leu33	8.110	4.064	1.339	$C^{\gamma}H$ (1.339) $C^{\delta}H_3$ (0.581)

Chemical shifts are expressed in p.p.m. relative to internal 2, 2-dimethyl-2-siapentane-5-sulfonate.
The sample was maintained at 5°C and pH 7.0.

dihedral angles, and 8 hydrogen-bond restraints were used. Cross-peak volumes were classified as strong, medium, or weak, corresponding to upper bound interproton distance restraints of 2.7, 3.3 and 5.0 Å, respectively (Cho *et al*., 2003). Backbone dihedral restraints inferred from $^3J_{HN\alpha}$ coupling constants were used as -55 ± 5^o for a $^3J_{HNa}$ of less than 6 Hz (Wagner *et al*., 1987; Driscoll *et al*., 1989). Three-dimensional structures were calculated using hybrid distance geometry and the dynamic simulated annealing protocol, as previously described (Nilges *et al*., 1988a; Nilges *et al*., 1988b; Nilges *et al*. 1988c; Driscoll *et al*., 1989), using the CNS 1.0 program on a SGI Indigo^2 workstation. The methodology employed was similar to the original protocol of Lee *et al*. (1994). Final structures were analyzed using PROCHECK (Lakovski *et al*., 1993) and displayed using the Insight II (Accelrys Inc., San Diego, USA) and MOLMOL programs (Koradi *et al*., 1996).

Results and Discussion

Circular dichroism spectroscopy CD spectra of human orexin-A were acquired at various pHs, temperatures, and solvent conditions. CD spectra in aqueous solutions were measured at a peptide concentration of 80 μM in 50 mM potassium phosphate. Fig. 2A shows that orexin-A contains a helical conformation in a physiological environment (pH 7.0, 298 K) by ellipticity at 222 nm. pH and temperature differences were not significant factors of helicity. However, in membrane mimetic conditions (in DPC) the helicity of human orexin-A increased (Fig. 2B). From the above results samples in 90% H_2O/10% D_2O (pH 7.0) and in 50 mM DPC/ 90% H_2O/10% D_2O (pH 7.0) solution were prepared for NMR experiments. But since the sample in 50 mM DPC solution showed problems like line broadening and an insufficient number of peaks in the TOCSY spectrum, only the sample in the physiological environment (90% H_2O/10% D_2O, pH 7.0, 278 K) was used for NMR.

NMR resonance assignments and secondary structures Complete proton resonance assignments for human orexin-A were achieved using the standard sequential resonance assignment procedure. Once the individual spin systems had been classified, the backbone sequential resonance assignment was completed by $d_{\alpha N}$ (i, i + 1) NOE connectivities in the 2D-NOESY spectrum. The chemical shifts of orexin-A are listed in Table 1 (BMRB code: 5994). A number of well-resolved intense d_{NN} cross-peaks from Cys^{12} to Thr^{32} were observed, suggesting the presence of an α-helix. Figure 3 summarizes the sequential and short-range NOE connectivities observed for human orexin-A in H_2O solution. The observations of continuous d_{NN} (i, i + 1) contacts and the characteristic $d_{\alpha N}$ (i, i + 3) and $d_{\alpha\beta}$ (i, i + 3) NOEs strongly support the existence of a-helices comprised of residues Cys^{14}-His^{21} (helix I) and

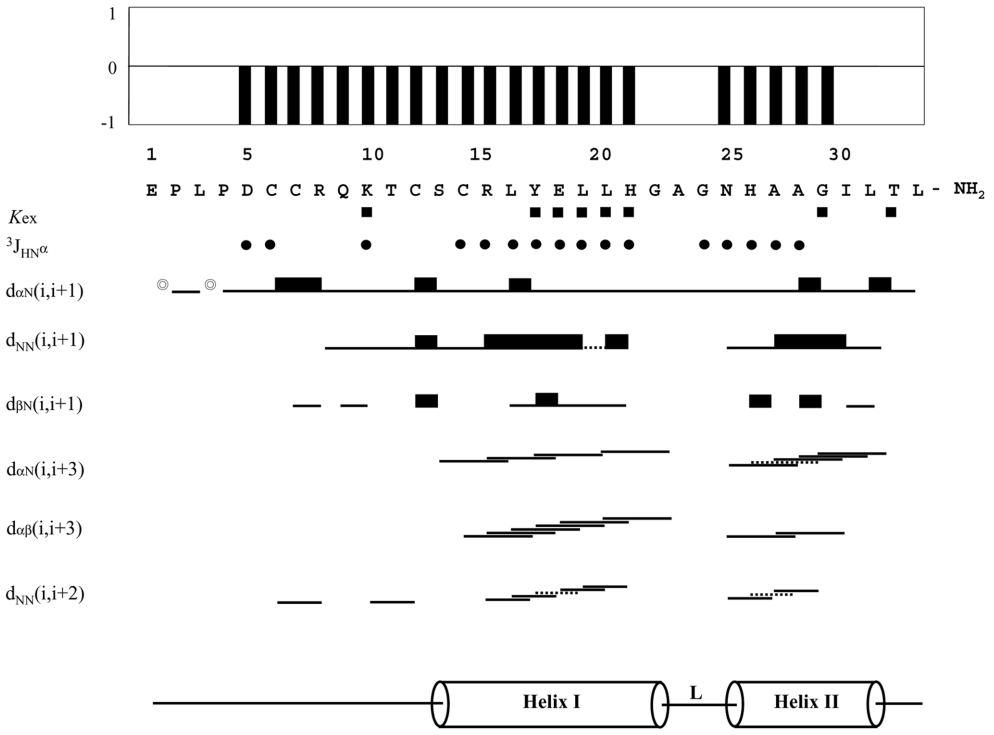

Fig. 3. Summary of NMR data for human orexin-A collected in H_2O, at 278 K, showing sequential and short-range NOE contacts. Slowly exchanging amide protons (■), backbone vicinal coupling constants (●; $^3J_{HN\alpha}$ < 6 Hz), and chemical shift indices (CSI) for the $C_{\alpha H}$ chemical shift are indicated. ◎ represents the proline residues that have been assigned to be trans-conformers based on characteristic $d_{\alpha\delta}$(i, i+1) NOEs. The dashed line represents the ambiguous NOEs from the resonance overlapping.

Asn[25]-Leu[31] (helix II) in H_2O solution. In particular, most $d_{\alpha N}$ (i, i + 3) and d_{NN} (i, i + 2) NOEs were observed for helix I and helix II. This result is further supported by the small $^3J_{HN}$ coupling constants, backbone amid-proton exchange data (Wishart *et al*., 1992), and chemical shift index values (Kane *et al*., 2000). The N-terminal Asp[5]-Thr[13] region was first predicted to be a helix by CSI data, and this was supported by a rigid turn conformation induced by disulfides bonds between Cys[6] and Cys[12], Cys[7] and Cys[14] was then found by structure calculation.

Structure-function of human orexin-A The NMR structure

Table 2. Structural statistics for the 20 final simulated-annealing structures of human orexin-A

	$<SA>_k$	$<\overline{SA}>_{kr}$
(A) rmsd from experimental distance restraints (Å)		
all (211)	0.0196	0.0212
sequential (| i − j | = 1) (78)	0.0152	0.0203
short range (1 < | i j | ≤ 5) (38)	0.0156	0.0130
intra residue (95)	0.0212	0.0242
hydrogen bond (8)	0.0122	0.0046
(B) rmsd from experimental dihedral restraints (deg)		
dihedral restraints (deg)	0.0820	0.1547
(C) Energies		
E_{total} (kcal · mol^{-1})	42.22	37.97
E_{NOE} (all) (kcal · mol^{-1})	6.76	7.58
E_{tor} (kcal · mol^{-1})	22.42	20.21
E_{repel} (kcal · mol^{-1})	10.08	7.79
E_{L-J} (kcal · mol^{-1})[a]	-121.761	-130.749
(D) Deviations from idealized covalent geometry		
bonds (Å)	0.0019	0.0020
angles (deg)	0.4013	0.3823
impropers (deg)	0.1544	0.1075

(E) Atomic rmsds[b]	Backbone atoms (nm)	All atoms (nm)
$<SA>_k$ vs $<\overline{SA}>_k$	0.039 (0.047)	0.157 (0.142)
$<\overline{SA}>_{kr}$ vs $<\overline{SA}>_k$	0.020 (0.046)	0.106 (0.091)
$<SA>_k$ vs $<\overline{SA}>_{kr}$	0.039 (0.049)	0.151(0.143)

$<SA>_k$, $<\overline{SA}>_k$, and $<\overline{SA}>_{kr}$ denote simulated-annealing structures, average structure of 20 calculated structures, and average restraint energy minimization structure, respectively.

[a]E_{L-J} is the Lennard-Jones/Van der Waals potential calculated using CHARMm empirical energy function.

[b]Values calculated in the Cys[14]-His[21] and Asn[25]-Leu[31] ranges are in parentheses.

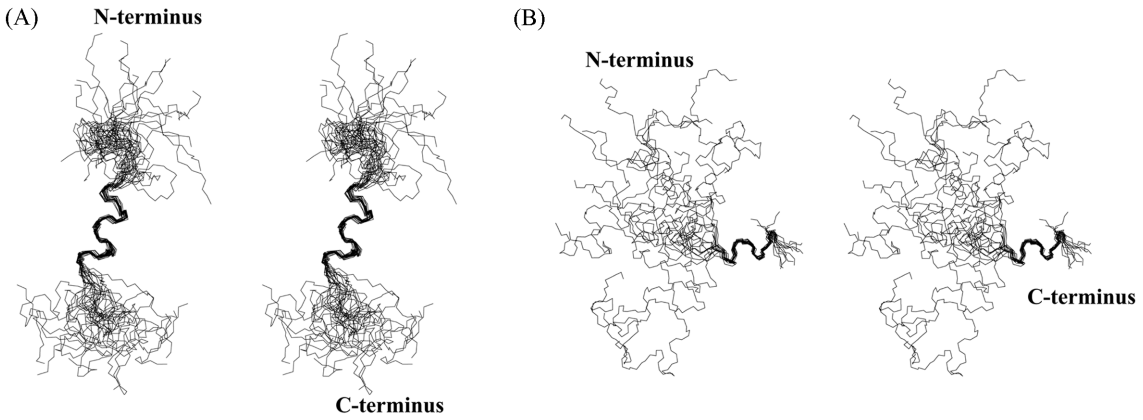

Fig. 4. Superimposition of the backbone atoms of 20 structures (C^α traces). The structures of human orexin-A were aligned for the best overlap of residues (A) 14-21 (Helix I) (B) 25-31 (Helix II), respectively.

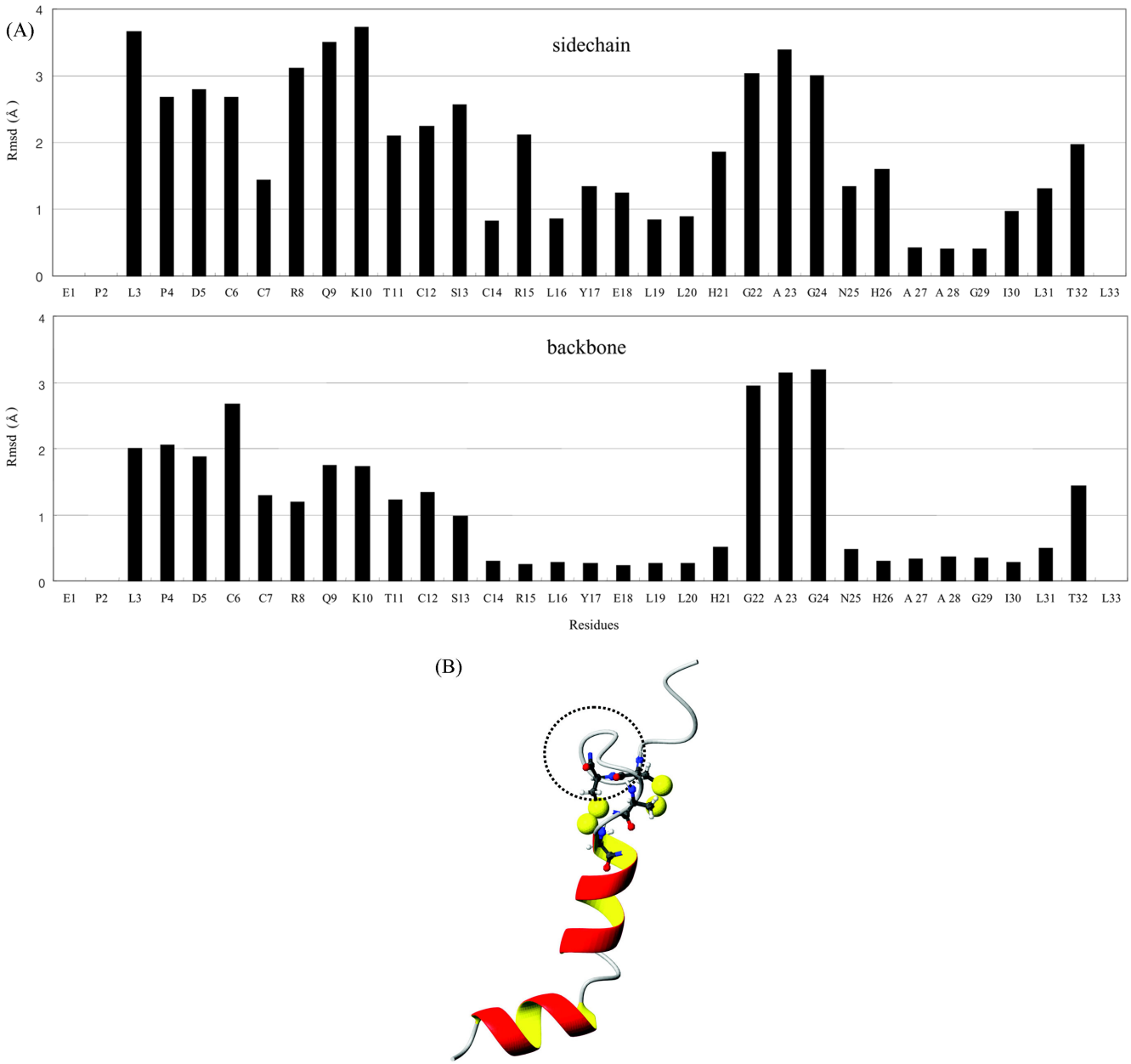

Fig. 5. (A) Atomic distribution of the average rmsds of the backbone and sidechain atoms in the 20 final simulated-annealing structures of human orexin-A. Deviations were calculated from the mean structure for the human orexin-A at pH 7.0, 278 K. (B) The average REM ribbon drawing structure of human orexin-A in H_2O. The figure was generated using the MOLMOL program. Grey circles were represented s-s bond and dashed line showed RQKT loop.

of human orexin-A (PDB code: 1R02) was calculated using the experimental restraints derived from 2D-NOESY and DQF-COSY spectra collected at 278 K. A total of 50 distance geometry structures served as starting structures for dynamical simulated-annealing calculations for the peptide in H_2O solutions. All 50 structures showed no restraint violations of greater than 0.5 Å for distances and 3° for torsion angles. The 20 lowest energy structures ($<SA>_k$) of the 50 simulated-annealing structures were selected for detailed structural analysis. The average structure ($<\overline{SA}>_k$) was calculated from the geometrical average of 20 $<SA>_k$ structure coordinates, and this was subjected to restraint energy minimization to correct covalent bonds and angle distortions. Table 2 summarizes the statistics of the final structures. The Ramachandran plot (not shown) for all 20 $<SA>_k$ structures showed that the ϕ, ψ angles of the final simulated-annealing structures were distributed properly in energetically acceptable regions. PROCHECK analysis then showed that all residues were in allowed regions of the Ramachandran map. The energies and structural statistics of the 20 $<SA>_k$ and the

$<\overline{SA}>_{kr}$ structure are listed in Table 2. A best-fit superposition of the 20 $<SA>_k$ structures and the energy-minimized average structure ($<\overline{SA}>_{kr}$) is shown in Fig. 4A, B. In Fig. 5A, the atomic rmsds of the final 20 structures for the individual residues are displayed with respected to the average structure (<SA>k).

The main structural features of human orexin-A are two a-helices spanning residues Cys^{14}-His^{21} (helix I) and Asn^{25}-Leu^{31} (helix II) in solution. Helix I was observed to be more compact than helix II. The two α-helices are connected by a flexible loop. The structure contains two intramolecular disulfide bonds between residues Cys^6 and Cys^{12}, and Cys^7 and Cys^{14} in its N-terminus (Fig. 5B) and these bonds make a rigid turn conformation between the Arg^8-Thr^{11} residues. Human orexin-A and human orexin-B have similar structures, so orexin receptors bind both orexin peptides (Kane *et al*., 2000). On comparing the two peptide structures, the residues of the $Cys^{14}His^{21}$ (helix I) of human orexin-A are well superposed with those of Gly^9Gly^{16} of human orexin-B, showing an rmsd of 0.8 Å for C^a atoms.

Both receptors, *h*OX1R (425 residues) and *h*OX2R (444 residues), belong to the class I subfamily within the superfamily of G-protein coupled receptors. They have identical conformations in the transmembrane, extra cellular loop, and the intra cellular loop 1, 2 regions. However, the N-terminal extra cellular domain, intracellular loop 3, and the C-terminal cytosolic domains have different conformations (Voisin *et al*., 2003). Thus, the N-terminal extra cellular domain of *h*OX1R might distinguish human orexin-A and human orexin-B. From studies on canine narcolepsy, the C-terminal region of human orexin-A, a region identical with human orexin-B, is essential for *h*OX2R activation (Wieland *et al*., 2002). However, in the case of human orexin-A, the binding affinity of human orexin-A without residues 1-14, showed 60-fold lower affinity for *h*OX1R, and 23-fold lower affinity for *h*OX2R. Human orexin-A without disulfide bonds showed similar results. These bonds were reported to play a key role in the stimulation of gastric acid secretion (Okumura *et al*., 2001). The rigid turn induced by the two disulfide bonds contains characteristic charged residues, RQKT. Although there is insufficient information about the interaction of this turn and receptors, it is apparent from a previous peptide mutation study (Voisin *et al*., 2003) that the N-terminal extra cellular domain of *h*OX1R might interact with the turn of human orexin-A and enhance the receptor binding affinity of human orexin-A. Moreover, breakage of these disulfide bonds might disrupt the turn conformation and induce lower binding human orexin-A affinity. In addition, a study of the E54K mutation in *h*OX2R (Hungs *et al*., 2001) suggested that the N-terminal extra cellular domain of *h*OX receptors might also interact with the C-terminal of orexin peptides. In conclusion, whereas the C-terminal helix region of orexin peptides might be essential for interaction with *h*OX receptors, the N-terminal region Glu^1-Cys^{12}, a rigid turn with a coil, of human orexin-A might potently increase its selectivity for *h*OX1R.

The helical wheel diagram shows that the hydrophobic residues (Leu^{16}, Leu^{19}, and Leu^{20}) are positioned on one side of the helix, while the hydrophilic residues (Cys^{14}, Arg^{15}, Tyr^{17}, Glu^{18}, and His^{21}) are located on the other side. There is accumulating evidence that many hormones display amphiphilic secondary structures, mainly α-helices. These kinds of amphiphilic peptides have the ability to self-aggregate or dimerize (Mirjam *et al*., 2002), but the data from the analytical ultra centrifuge analysis showed that the monomer form predominated under the NMR experimental condition.

Human neuropeptide Y, are orexin-like signaling peptide, is negatively regulated by leptin (Zarjevski *et al*., 1993; Stephens *et al*., 1995), and has been characterized as one of the positive regulators of feeding behavior. Monks *et al.* (1996) suggested that the monomeric human neuropeptide Y molecule could be associated with the hydrophobic side in the α-helical region at high concentration, and that it might even form a dimer (Mirjam *et al*., 2002). But in our study, the monomeric form dominated and the structure of monomeric form was elucidated. It is interesting to note that the solution structure of human neuropeptide Y also contains a kink in the middle of amphiphilic helix (Monks *et al*., 1996). Schwartz *et al.* (1998) proposed that the orexins play a role analogous to that of neuropeptide Y in the control of energy balance. Even though orexins and neuropeptide Y share low sequence homology, we can presume that their similar biological functions stem from the structural homology between the two neuropeptides. Interestingly, the human orexin-A cappinghelix conformation induced by disulfide bonds extends duration of action versus neuropeptide Y (Willie *et al*., 2001).

In this study, we demonstrate the solution structure of human orexin-A and compared this with human orexin-B. Like other neuropeptides, its conformation shows an amphiphilic helix with a unique RQKT turn. In our future work, the interaction between orexin peptides and receptors will be further studied. We hope to obtain more detailed information on orexin-receptor interaction for novel drug development.

Acknowledgments This study was supported by the Korean Ministry of Science and Technology and the Korean Science and Engineering Foundation through the NRL program of MOST NRDP (M1-0203-00-0020).

References

Bernardis, L. L. and Bellinger, L. L. (1993) The lateral hypothalamic area revisited: Neuroanatomy, body weight regulation. *Neurosci. Biobehav. Rev.* **17**, 141-193.

Bernardis, L. L. and Bellinger, L. L. (1996) The lateral hypothalamic area revisited: Ingestive behavior. *Neurosci. Biobehav. Rev.* **20**, 189-287.

Cho, M. K., Kim, S. S., Lee, M. R., Shin, J., Lee, J., Lim, S. K.,

Baik, J. H., Yoon, C. J., Shin, I. and Lee, W. (2003) NMR studies on turn mimetic analogs derived from melanocyte-stimulating hormones. *J. Biochem. Mol. Biol.* **36**, 552-557.

Darbon, H., Bernassau, J. -M., Deleuze, C., Chenu, J., Roussel, A. and Cambillau, C. (1992) Solution conformation of human neuropeptide Y by ^{1}H nuclear magnetic resonance and restrained molecular dynamics. *Eur. J. Biochem.* **209**, 765-771.

Davis, D. G. and Bax, A. (1985) Assignment of complex ^{1}H NMR spectra via two-dimensional homonuclear Hartmann-Hahn spectroscopy. *J. Am. Chem. Soc.* **107**, 2820-2821.

Delaglio, F., Grzesiek, S., Vuister, G. W., Zhu, G., Pfeifer, J. and Bax, A. (1995) NMRPipe: a multidimensional spectral processing system based on UNIX pipes. *J. Biomol. NMR*, ***6***, 277-293.

Driscoll, P. C., Gronenborn, A. M. and Clore, G. M. (1989) The influence of stereospecific assignments on the determination of three-dimensional structures of proteins by nuclear magnetic resonance spectroscopy: Application to the sea anemone protein BDS-1. *FEBS Lett.* **243**, 223-233.

Driscoll, P. C., Gronenborn, A. M., Beress, L. and Clore, G. M. (1989) Determination of the three-dimensional solution structure of the antihypertensive and antiviral protein BDS-1 from the sea anemone *Anemonia sulcata*: A study using nuclear magnetic resonance and hybrid distance geometry-dynamical simulated annealing. *Biochemistry* **28**, 2188-2198.

de Lecea, L., Kilduff, T. S., Peyron, C., Gao, X., Foye, P. E., Danielson, P. E., Fukuhara, C., Battenberg, E. L., Gautvik, V. T., Bartlett, F. S. 2nd, Frankel, W. N., van den Pol, A. N., Bloom, F. E., Gautvik, K. M. and Sutcliffe, J. G. (1998) The hypocretins: Hypothalamus-specific peptides with neuroexcitatory activity. *Proc. Natl. Acad. Sci. USA* **95**, 322-327.

De Wied, D. and Croiset, G. (1991) Stress modulation of learning and memory processes. *Methods Achieve Exp. Pathol.* **15**, 167-199.

Fan, W., Boston, B. A., Kesterson, R. A., Hruby, V. J. and Cone, R. D. (1997) Role of melanocortigergic neurons in feeding and the *agouti* obesity syndrome. *Nature* **385**, 165-168.

Goddard, D. and Kneller, D. G. (2003) SPARKY 3, University of California, San Francisco, http://www.cgl.ucsf.edu/home/sparky/

Hungs, M., Fan, J., Lin, L., Lin, X., Maki, R. A. and Mignot, E. (2001) Identification and functional analysis of mutations in the hypocretin (orexin) genes of narcoleptic canines. *Genome Res.* **11**, 531-539.

Jeener, J., Meier, B. H., Bachman, P. and Ernst, R. R. (1979) Investigation of exchange processes by two-dimensional NMR spectroscopy. *J. Chem. Phys.* **71**, 4546-4553.

Kane, J. K., Tanaka, H., Parker, S. L., Yanagisawa, M. and Li, M. D. (2000) Sensitivity of orexin-A binding to phospholipase C inhibitors, neuropeptide Y, and secretin. *Biochem. Biophys. Res. Commun.* **272**, 959-965.

Koo, B. K., Kim, M. H., Lee, S. T. and Lee, W. (2002) Purification and spectroscopic characterization of the human protein tyrosine kinase-6 SH3 domain. *J. Biochem. Mol. Biol.* **35**, 343-347.

Koradi, R., Billeter, M. and Wüthrich, K. (1996) MOLMOL: A program for display and analysis of macromolecular structures. *J. Mol. Graphics* **14**, 51-55.

Lakovski, R. A., MacArthur, M. W., Moss, D. S. and Thornton, J. M. (1993) PROCHECK: A program to check the stereochemical quality of proteins structures. *J. Appl. Crystallogr.* **26**, 283-291.

Lee, J.-H., Bang, E. J., Chae, K.-J., Kim, J. Y. Lee, D. W. and Lee, W. (1999) Solution structures of a new hypothalamic neuropeptide, human hypocretin-2/orexin-B. *Eur. J. Biochem.* **266**, 831-839.

Lee, W., Moore, C. H., Watt, D. D. and Krishna, N. R. (1994) Solution structure of the variant-3 neurotoxin from *Centruroides sculpturatus* Ewing. *Eur. J. Biochem.* **218**, 89-95.

Li, S. J., Varga, K., Archer, P., Hruby, V. J., Sharma, S. D., Kesterson, R. A., Cone, R. D. and Kunos, G. (1996) Melanocortin antagonists define two distinct pathways of cardiovascular control by α- and γ-melanocyte-stimulating hormones. *J. Neurosci.* **16**, 5182-5188.

Marion, D. and Wuthrich, K. (1983) Application of phase sensitive two-dimensional correlated spectroscopy (COSY) for measurements of ^{1}H-^{1}H spin-spin coupling constants in proteins. *Biochem. Biophys. Res. Commun.*, **113**, 967-974.

Merutka, G., Dyson, H. J. and Wright, P. E. (1995) Random coil ^{1}H chemical shifts obtained as a function of temperature and trifluoroethanol concentration for the peptide series GGXGG. *J. Biomol. NMR* **5**, 14-24.

Mirjam, L., Verena, G., Reto, B., Barbara, C., Gerd, F. and Oliver, Z. (2002) Bovine pancreatic polypeptide (bPP) undergoes significant changes in conformation and dynamics upon binding to DPC micelles. *J. Mol. Biol.* **322**1117-1133.

Monks, S. A., Karagianis, G., Howlett, G. J. and Norton, R. S. (1996) Solution structure of human neuropeptide Y. *J. Biomol. NMR* **8**, 379-390.

Murphy, M. T., Richards, D. B. and Lipton, J. M. (1983) Antipyretic potency of centrally administered α-melanocyte stimulating hormone. *Science* **221**, 192-193.

Nakabayashi, M., Suzuki, T., Takahashi, K., Totsune, K., Muramatsu, Y., Kaneko, C., Date, F., Takeyama, J., Darnel, A. D., Moriya, T. and Sasano, H. (2003) Orexin-A expression in human peripheral tissues. *Mol Cell Endocrinol.* **205**, 43-50.

Nilges, M., Clore, G. M. and Gronenborn, A. M. (1988a) Determination of three-dimensional structures of proteins from interproton distance data by hybrid distance geometry-dynamical simulated annealing calculations. *FEBS Lett.* **229**, 317-324.

Nilges, M., Clore, G. M. and Gronenborn, A. M. (1988b) Determination of three-dimensional structures of proteins from interproton distance data by dynamical simulated annealing from a random array of atoms. Circumventing problems associated with folding. *FEBS Lett.* **239**, 129-136.

Nilges, M., Gronenborn, A. M., Brunger, A. T. and Clore, G. M. (1988c) Determination of three-dimensional structures of proteins by simulated annealing with interproton distance restraints. Application to crambin, potato carboxypeptidase inhibitor and barley serine proteinase inhibitor 2. *Protein Eng.* **2**, 27-38.

Okumura T., Takeuchi S., Motomura W., Yamda H., Egashira S. I., Asahi S., Kanatani A., Ihara M. and Kohgo Y. (2001) Reauirement of intact disulfide bonds in orexin-A induced stimulation of gastric acid secretion that is mediated by OX1 receptor activation. *Biochem. Biophys. Res. Commun.* **280**, 976-981.

Piotto, M., Saudek, V. and Sklenar, V. (1992) Gradient-tailored excitation for single-quantum NMR spectroscopy of aqueous solutions. *J. Biomol. NMR*, **2**, 661-665.

Rance, M., Sorensen, O. W., Bodenhausen, G., Wagner, G., Ernst,

R. R. and Wüthrich, K. (1983) Improved spectral resolution in COSY ^{1}H-NMR spectra of proteins via double quantum filtering. *Biochem. Biophys. Res. Commun.*, **117**, 479-485.

Sakurai, T., Amemiya, A., Ishii, M., Matsuzaki, I., Chemelli, R. M., Tanaka, H., Williams, S. C., Richardson, J. A., Kozlowski, G. P., Wilson, S., Arch, J. R. S., Buckingham, R. E., Haynes, A. C., Carr, S. A., Annan, R. S., McNulty, D. E., Liu W. S., Terrett, J. A., Elshourbagy, N. A., Bergsma, D. J. and Yanagisawa, M. (1998) Orexins and orexin receptors: A family of hypothalamic neuropeptides and G protein-coupled receptors that regulate feeding behavior. *Cell* **92**, 573-585.

Schwartz, M. W. (1998) The big picture of energy homeostasis gets a little bigger. *Nat. Med.* **4**, 385-386.

Smith, E. M., Hughes, T. K., Hashemi, F. and Stefano, G. B. (1992) Immunosuppressive effects of corticotropin and melanotropin and their possible significance in human immunodeficiency virus infection. *Proc. Natl. Acad. Sci. USA* **89**, 782-786.

Stephens, T. W., Basinski, M., Bristow, P. K., Bue-Valleskey, J. M., Burgett, S. G., Craft, L., Hale, J., Hoffmann, J., Hsiung, H. M., Kriauciunas, A., Mackellar, W., Rosteck, P. R., Schoner, B., Smith, D., Tinsley, F. C., Zhang, X.-Y. and Heiman, M. (1995) The role of neuropeptide Y in the antiobesity action of the obese gene product. *Nature* **377**, 530-532.

Voisin, T., Rouet-Benzineb, P., Reuter, N. and Laburthe, M. (2003) Orexins and their receptors: structural aspects and role in peripheral tissues. *Cell. Mol. Life. Sci.* **60**, 72-87.

Wagner, G., Braun, W., Havel., T. F., Schaumann, T., Go, N. and Wuthrich, K. (1987) Protein structures in solution by nuclear magnetic resonance and distance geometry: The polypeptide fold of the basic pancreatic trypsin inhibitor determined using two different algorithms, DISGEO and DISMAN. *J. Mol. Biol.* **196**, 611-639.

Werner, K., Clemens, B., Paul, G. and Hans S. (1993) Determination of the disulphide bonding pattern in proteins by local and global analysis of nuclear magnetic resonance data. Application to flavoridin. *J. Mol. Biol.* **232**, 897-906.

Wieland, H. A., Soll, R. M., Doods, H. N., Stenkamp, D., Hurnaus, R., Lammle, B. and Beck-Sickinger, A. G. (2002) The SK-N-MC cell line expresses an orexin binding site different from recombinant orexin 1-type receptor. *Eur. J. Biochem.* **269**, 1128-1135.

Willie, J. T., Chemelli, R. M., Sinton, C. M. and Yanagisaw, M. (2001) To Eat or To Sleep? Orexin in the Regulation of Feeding and Wakefulness. *Annu. Rev. Neura, Osci*. **24**, 429-458.

Wishart, D. S., Sykes, B. D. and Richards, F. M. (1992) The chemical shift index: A fast and simple method for the assignment of protein secondary structure through NMR spectroscopy. *Biochemistry* **31**, 1647-1651.

Zarjevski, N., Cusin, I., Vettor, R., Rohner-Jeanrenaud, F. and Jeanrenaud. (1993) Chronic intracerebroventricular neuropeptide-Y administration to normal rats mimics hormonal and metabolic changes of obesity. *Endocrinology* **133**, 1753-1758.